Systematic measurements of dose-dependent responses for combinatorial treatments of SA and JA led to the development of transcriptomic biomarkers

Atsuki Tomita[1,2], Taro Maeda[1], Natsumi Mori-Moriyama[3], Yasuyuki Nomura[3], Yuko Kurita[4], Makoto Kashima[5], Shigeyuki Betsuyaku[6], Atsushi J. Nagano[1, 7*]

[1] Institute for Advanced Biosciences, Keio University, Tsuruoka, Yamagata 997-0052, Japan

[2] Graduate School of Media and Governance, Keio University, Fujisawa, Kanagawa 252-0882, Japan

[3] Research Institute for Food and Agriculture, Ryukoku University, Otsu, Shiga 520-2194, Japan

[4] Graduate School of Life Sciences, University of Tokyo, Bunkyo-ku, Tokyo 113-8657, Japan

[5] Faculty of Science, Toho University, Funabashi, Chiba, 274-8510, Japan

[6] Faculty of Agriculture, Ryukoku University, Otsu, Shiga 520-2194, Japan

[7] Bioscience and Biotechnology Center, Nagoya University, Nagoya, Aichi, 464-8601, Japan

Corresponding Author:

Atsushi J. Nagano

Bioscience and Biotechnology Center, Nagoya University, Nagoya, Aichi, 464-8601, Japan

Email: anagano@agr.nagoya-u.ac.jp

ABSTRACT

Salicylic acid (SA) and jasmonic acid (JA) regulate plant defense against pathogens and herbivores. The SA-JA pathways often interact antagonistically with the induction of one, leading to the suppression of the other. However, the effect of combined SA/JA concentrations on plant responses is unknown. Here, we show transcriptional responses specific to combinations of SA and JA concentrations and develop transcriptomic biomarkers to estimate SA/JA response states. Combinatorial treatments with eight concentrations of SA and JA, combined with large-scale transcriptome analysis, revealed 43 different expression patterns, including not only well-known antagonistic responses but also responses specific to combinations of SA/JA concentrations. Notably, the expression of *CYP94B3*, a key enzyme involved in JA-Ile turnover, was finely tuned by specific SA/JA concentration combinations being induced under high SA conditions in a JA dose-dependent manner. In addition, the expression peaks of indole glucosinolate biosynthesis genes were found at approximately 30-fold higher JA concentrations than aliphatic glucosinolate biosynthesis genes. Furthermore, to quantitatively estimate SA/JA response states, we developed transcriptomic biomarkers using a machine learning approach. The marker specifically estimated response states to target phytohormones. Through analysis of *npr3/4* double mutants, we confirmed that the biomarkers were applicable to the analysis of mutants. The biomarkers will allow us to extract insights into phytohormone responses from various large-scale transcriptome data, e.g., field transcriptomics and single-cell RNA-Seq.

(219 / 250 words)

Keywords: Salicylic acid, Jasmonic acid, transcriptome, biomarker

Running head: Transcriptome analysis of response to SA/JA concentration in *A.thaliana*

INTRODUCTION

When plants suffer environmental stresses, they produce various phytohormones that regulate resistance mechanisms. The plants respond to a wide range of biotic stresses through the production of salicylic acid (SA) and jasmonic acid (JA). Salicylic acid (SA) is a phytohormones required for plant defense against pathogens (Maruri-López et al., 2019). Pathogen infection induces biosynthesis of SA in infected tissues (Mishina and Zeier, 2007). SA-responsive genes include pathogenesis-related (PR) proteins that have antimicrobial properties (Jain and Khurana, 2018). Phytohormone regulate various physiological processes in plants at nanomolar concentrations (Munné-Bosch and Müller, 2013). SA response is an example of a response altered by quantitative concentrations. When intracellular SA levels are high, the SA receptors, NPR3 and NPR4, induce programmed cell death that prevents the establishment of parasitism(Dodds and Rathjen, 2010; Fu et al., 2012). Jasmonic acid (JA) is a phytohormones synthesized against insects and necrotrophic pathogens (Ghorbel et al., 2021; Wasternack and Hause, 2013). The JA pathway, induced by signals from insect saliva and damaged cells, promotes widespread insect resistance (Howe and Jander, 2008). JA induces glucosinolate (GSL) biosynthesis (Fritz et al., 2010; Guo et al., 2013). In Brassicaceae, GSLs are chemical defense substances that act directly against insects and microbes (Hopkins et al., 2009; Wittstock and Burow, 2010). It is known that different types of GSLs are induced depending on the type and timing of external threats (Abuyusuf et al., 2023).

The crosstalk between salicylic acid (SA) and jasmonic acid (JA) signaling pathways in plant defense is characterized by reciprocal antagonism (Hou and Tsuda, 2022; Thaler et al., 2012). This antagonism is likely adaptive, allowing plants to fine-tune their defense responses against different types of attackers (Pieterse et al., 2001; Pieterse and Dicke, 2007). In *Arabidopsis*, the regulatory protein NPR1 mediates the crosstalk by facilitating SA-induced suppression of JA signaling through its cytosolic function (Spoel et al., 2003). The

antagonistic interaction between SA and JA pathways can modulate the expression of defense genes and affect gene-for-gene resistance to pathogens. The JA-insensitive *coi1* mutation restored CMV(Y)-activated expression of SA-dependent PR genes in an SA-deficient background, demonstrating the complex interplay between these pathways(Takahashi et al., 2004). The interaction between SA and JA is generally antagonistic, but there are some exceptions. During effector-triggered immunity, simultaneous accumulation of SA and JA was observed, necessitating the activation of both signaling pathways (Kenton et al., 1999; Liu et al., 2016; Tsuda et al., 2009). Interaction of SA and JA signaling pathways can also result in synergistic defense and oxidative stress effects leading to cell death (Mur et al., 2006; Zhang et al., 2020). Furthermore, simultaneous activation of SA-dependent systemic acquired resistance and JA-dependent induced systemic resistance has been shown to have additive effects on induced defense against pathogens (Niu et al., 2011; Van Wees et al., 2000). Cooperative interactions between SA and JA have been frequently observed. However, their detailed mechanisms remain unclear. SA and JA signaling levels are controlled by the plant itself and manipulated by external enemies (Spoel et al., 2007). For example, *Pseudomonas syringae* promotes pathogenicity by producing coronatine that mimic jasmonic acid isoleucine (Zheng et al., 2012). Herbivores also manipulate SA and JA signaling levels using salivary enzymes to weaken plant wounding responses (Weech et al., 2008). It is suggested that SA and JA signaling levels are altered by both the plant's own responses and external enemies' manipulation. To fully understand the complex interplay of SA/JA signaling pathways, it is important to analyze the plant's response to a range of SA and JA concentrations and their combinations.

Systematic transcriptome analysis using the various combinations of SA and JA concentrations is essential for a comprehensive understanding of SA-JA crosstalk (Robert-Seilaniantz et al., 2011). Although, there are several small-scale studies that have measured the dose response of SA and JA (Hickman et al., 2019; Mur et al., 2006; Zhang et al., 2020),

most previous studies on SA-JA crosstalk have been comparisons between with and without treatment. Because massive RNA-Seq experiments are required, it is challenging to systematically analyze the various combinations of SA and JA concentrations. On the other hand, various high-throughput RNA-Seq library preparation methods have been proposed (Bjornson et al., 2020; Kamitani et al., 2019; Kashima et al., 2020; Santacruz et al., 2022). Using such technical advances, large-scale transcriptome projects emerged in recent years. For example, effects of temperature, daylength and circadian clock were systematically analyzed using rice seedlings (Hashida et al., 2024). The data enhanced the model to predict transcriptome dynamics under complex field conditions.

In this study, we systematically analyzed plant responses to combinations of various SA/JA concentrations and developed a transcriptomic biomarker for SA/JA. We treated *A. thaliana* seedlings with 64 combinations of SA and JA concentration and quantified transcriptomes using high-throughput RNA-seq (Kamitani et al., 2019; Kashima et al., 2020). The systematic data enable us not only to revealed the diverse responses of genes to SA/JA concentrations but also to create a transcriptomic biomarker that specifically estimates SA/JA response states.

RESULTS

Expression topography of SA/JA responses revealed by high-throughput RNA-seq

In order to evaluated how SA/JA concentration affects the interaction between the SA and JA signaling pathways, we performed transcriptome profiling of *A. thaliana* seedlings treated for 6 hours to 64 different SA/JA concentrations combinations (Fig. 1A, B, Supplementary Table S1). We employed an assay system that allows the simultaneous processing of 96 samples using 96-well plates (Fig. 1A, B). We used at least four biological replicates per a treatment condition for RNA-seq. In total, 384 samples were processed. 370 samples with more than $10^{5.5}$ reads were used for further analysis (Supplementary Fig. S1A, B). The 12,963 genes with an average expression level higher than 1.5 on the log2(RPM+1) scale were designated as expressed genes and used for further analysis (Supplementary Fig. S1A, C). In this study, a gene expression pattern by SA/JA concentration was called an expression topography (Fig. 1C-F).

We evaluated the expression topography of well-known marker genes involved in the SA/JA response, as well as two genes associated with JA metabolism. The marker gene for the SA response, *PR1*, exhibited an expression threshold at 0.033 mM SA. When JA was treated with 1 mM, the expression of *PR1* was completely suppressed. The optimal concentration of SA for *PR1* expression was 0.33 mM (Fig. 1C, Supplementary Fig. S2A). The marker gene for the JA response, *VSP1*, exhibited an expression threshold at 0.001 mM JA. The optimum concentration of JA for *VSP1* expression was 0.1 mM (Fig. 1D, Supplementary Fig. S2B). These results are consistent with the qualitative understandings of SA/JA responses and SA and JA antagonism in previous studies (Hou and Tsuda, 2022; Mur et al., 2006; Spoel et al., 2003; Thaler et al., 2012). Figure 1E shows the expression of *LOX3*, which was increased under 0mM to 0.33mM JA conditions in a JA concentration-dependent manner. *LOX3*

encodes the enzyme for the first step of JA synthesis (Chauvin et al., 2016). JA biosynthesis in plants exhibits a positive feedback loop with the pathway including key enzymes such as *LOXs* upregulated dose-dependently by JA (Yang et al., 2020). The increase of *LOX3* expression in response to JA concentrations ranging from 0 to 0.33 mM is consistent with previous studies showing a positive feedback loop in JA biosynthesis. Interestingly, *LOX3* expression was suppressed under 1 mM SA/JA treatment, suggesting that the positive feedback loop of *LOX3* is terminated once JA/SA levels reach substantial accumulation (Fig. 1. E, Supplementary Fig. S2C). In contrast, the expression of *CYP94B3*, a key regulator in the suppression of the JA signaling cascade, decreased in a JA concentration-dependent manner (Fig. 1F, Supplementary Fig. S2D). CYP94B3 oxidizes the bioactive form of JA, jasmonoyl-L-isoleucine (JA-Ile). This oxidation by CYP94B3 regulates JA signaling levels and could affect SA/JA crosstalk (Kitaoka et al., 2014; Koo et al., 2011). Interestingly, *CYP94B3* expression was most upregulated under high SA conditions, showing a 4.6-folds increase between 0 mM and 1 mM SA in the presence of 1 mM JA.

To visualize transcriptome-wide characteristics in response to SA and JA treatments, we conducted a principal component analysis (PCA) and detection of differentially expressed genes (DEGs). The PCA was performed on 370 samples with expressed genes. The principal component 1 explained 19.3% of variance and coordinated with the SA treatment concentrations (Fig. 1G, Supplementary Fig. S3A). The principal component 2 explained 6.7% of variance and coordinated with the JA treatment concentrations (Fig. 1H, Supplementary Fig. S3B). No apparent differences were observed among the 96 well plates (Fig. 1I, Supplementary Fig. S3C-F). The number of DEGs between control and phytohormone-treated samples increased in a dose-dependent manner for SA and JA (Supplementary Fig. S4A-C). For both SA and JA, there was a larger number of up-regulated genes than down-regulated genes in most conditions from the 0 mM to 0.33 mM treatments

(Supplementary Fig. S4D). In contrast, the number of down-regulated genes exceeded that of up-regulated in the 1 mM treatment.

Expression topography revealed diverse responses of genes to SA/JA concentrations

3,001 genes whose expression varied with the treatment of SA/JA were selected as SA/JA responsive genes (Supplementary Fig. S1A, D) and used for the following analysis. Each SA/JA responsive gene was normalized by Z-scoring and smoothed by a 3x3 moving average filter to extract key characteristics of the expression topography. We performed clustering of the SA/JA responsive genes by affinity propagation. The affinity propagation determined 43 clusters based on the expression topography (Fig. 2A). The clusters contained 23 – 299 genes. We found that genes with a similar pattern were enriched in clusters (Fig. 2B). Gene expression of cluster A-02 increased in a concentration-dependent manner in response to JA and decreased in a concentration-dependent manner in response to SA. On the other hand, gene expression of cluster C-01 increased in a concentration-dependent manner in response to SA and decreased in a concentration-dependent manner in response to JA. To classify the clusters to groups, hierarchical clustering was performed using Pearson's correlation coefficients among expression topographies of the clusters. The optimal number of groups was estimated, and the clusters were classified into group A to H (Fig. 2C). Group F was the largest group and had 1,435 genes, which was about half of the 3,001 SA/JA-affected genes. In contrast, the smallest group was the group G containing 74 genes (Fig. 2A). Group B had an expression topography that was up-regulated by high concentrations of SA and JA. By contrast, group F had an expression topography that was down-regulated by high concentrations of SA and JA. The expression of group D was enhanced at intermediate concentrations of SA and was not reduced by increasing JA concentrations.

Expression topographies are associated with gene functions

To examine whether genes with similar expression topographies shared biological functions, enrichment analysis was conducted on 43 clusters. Eighteen clusters were found to be enriched with 1-103 GO terms (adjusted $P < 0.05$, Fig. 3A, Supplementary Table. S2). Genes in cluster A-02 were enriched in GO terms "response to jasmonic acid" (GO:0009753, adjusted $P = 4.09 \times 10^{-4}$). This cluster contained many JA-responsive genes reported in previous studies, such as *VSP2*, *JAZ8*, *JAZ10* and *JOX3* (Fernández-Calvo et al., 2011). Cluster C-01 showed the expression induced by SA and suppressed by JA. The *PR1* gene was contained in this cluster. Multiple GO terms were enriched in cluster C-01, including "response to bacterium" (GO:0009617, adjusted $P = 1.18 \times 10^{-7}$) and "response to salicylic acid" (GO:0009751, adjusted $P = 3.55 \times 10^{-6}$). When both SA and JA were treated in high concentrations, genes in cluster B-01 were up-regulated and genes in clusters F-07 and F-08 were down-regulated. In cluster B-01, GO terms such as "protein folding" (GO:0006457, adjusted $P = 2.68 \times 10^{-5}$) and "response to reactive oxygen species" (GO:0000302, adjusted $P = 1.61 \times 10^{-3}$) were enriched. The cluster B-01 mainly comprised genes encoding heat shock proteins such as HSP17.4 and HSP17.6. Clusters F-07 and F-08 were enriched in GO terms such as "ribosome biogenesis" (GO: 0042254, adjusted $P = 7.71\times 10^{-30}$ and 5.31×10^{-4}) and "translation" (GO: 0006412, adjusted $P = 1.52 \times 10^{-75}$ and 3.28×10^{-2}). GO terms associated with "photosynthesis" (GO:0015979, adjusted $P = 1.57 \times 10^{-4}$ and 4.22×10^{-3}) were enriched in clusters F-05 and F-06. Genes in the clusters F-05 and F-06 were down-regulated in a dose-dependent and additive manner by SA/JA co-treatment (Fig. 3A). These results were consistent with previous studies, which demonstrated that co-treatment with SA and JA reduced the expression of photosynthesis-related genes (Hickman et al., 2019; Schweiger et al., 2014; Zhang et al., 2020).

Based on analysis of the expression topography, we found that two subtypes of GSLs were induced by different concentrations of JA. In cluster E-01, the GO term "glucosinolate

biosynthetic process" (GO:0019761, adjusted P = 5.32 x 10^{-3}) was significantly enriched (Fig. 3A). Interestingly, "glucosinolate biosynthetic process" was also significantly enriched in cluster F-02 (adjusted P = 8.22 x 10^{-3}). The cluster E-01 contained genes related to indole glucosinolate biosynthesis, *e.g. SUR1, CYP83B1, CYP79B3, MAM.* In contrast, the cluster F-02 contained genes related to aliphatic GSL biosynthesis, *e.g. MAM3, CYP79F2, BCAT4, SOT18*. The expression peak of indole GSL biosynthesis genes was found at lower concentration of JA than that of aliphatic GSL (Fig. 3B-K). In low SA concentrations (0 ~ 0.01 mM), the expression peaks of indole GSL biosynthesis genes were found around 0.1 mM JA (Fig. 3B). On the other hand, the expression peaks of aliphatic GSL biosynthesis genes were found around 0.003 mM JA (Fig. 3B). The expression peaks of indole GSL-related genes were found at approximately 30-fold higher JA concentrations than that of aliphatic GSL-related genes. This response was specific to low SA concentrations (Fig. 3C, Supplementary Fig. S5).

No single gene was a specific and quantitative SA/JA response marker

Our comprehensive dataset allowed us to systematically evaluate how the expression of a single gene correlated with treated concentrations of SA and JA (Fig. 4A, B, C, Supplementary Table. S3). *PR1* and *VSP1* have long been used as expression markers of SA and JA response (Javed et al., 2025; Zhang et al., 2020). Correlation coefficients between *PR1* and treatment concentrations of SA/JA were 0.63 and -0.30, respectively (Fig.4C). Correlation coefficients between *VSP1* and SA/JA treatment concentrations were -0.20 and 0.07, respectively (Fig.4C). *PR1* had the 29th highest correlation with SA concentration. On the other hand, *VSP1* had the 4,695th highest correlation with JA concentration. The genome-wide pattern of correlations indicated that correlations with SA and JA were associated with each other (fig. 4C). The gene with the highest correlation with SA treatment concentration was *HRG2*. The correlation with SA was 0.74 and that with JA was 0.14 (Fig. 4C, D). The

gene having the highest negative correlation with SA was *UL4Z*, with a correlation of -0.70 with SA and - 0.22 with JA (Fig. 4C, E). The gene with the highest positive correlation with JA treatment concentration was *AT2G47950*. The correlation with JA was 0.85 and that with SA was 0.16 (Fig. 4C, F). The gene having the highest negative correlation with JA was *SAUR6*, with a correlation of -0.68 with JA and -0.44 with SA (Fig. 4C, G). These four genes respond in a threshold manner to specific concentrations of SA/JA (Fig. 4D-G). These results showed difficulty in identifying a gene whose expression served as a specific and quantitative response marker.

Development of a transcriptomic biomarker of SA/JA response state

To overcome the limit of using a single gene as a response marker, we developed a transcriptomic biomarker of the SA/JA response state. This enabled the estimation of the SA/JA response state corresponding to a specific treatment concentration of SA/JA. To create a transcriptomic biomarker that correlated with SA/JA and uncorrelated with their counterpart, we employed the method using ensemble learning and L1-regularized linear regression, LASSO (Fig. 5A). The transcriptome data of 370 samples at 64 concentration conditions were used as training data. We also obtained additional transcriptome data of 101 samples at 25 conditions of SA and JA combining 5 concentrations: 0, 0.001, 0.01, 0.1, and 1 mM (Supplementary Fig. S6). The transcriptome data were used as test data for validating predictive performance of the markers. The predicted values of markers for the training data highly correlated with the treated concentrations of SA/JA (0.98 for SA and 0.98 for JA, Fig. 5B, C). For the test data, correlation coefficients between the predicted concentrations of the markers and the treated concentrations of their target phytohormones were 0.97 for SA and 0.96 for JA (Fig. 5D, E). These correlation coefficients were higher than the best correlated single genes (Fig. 4). As the treated concentration increased, the predicted concentration also gradually increased. However, in the high concentration range, the predicted concentrations

were underestimated. On the other hand, correlation coefficient between the predicted SA concentrations and the treated JA concentration was -0.11 (Fig. 5F), and correlation coefficient between the predicted JA concentrations and the treated SA concentration was 0.10 (Fig. 5G). These results showed that the transcriptomic biomarkers worked in a specific and, at least relatively, quantitative manner. Our ensemble learning approach allowed us to evaluate contributions of genes to the marker. To reveal the genes contributing the marker, we calculated the selection frequency of genes in the transcriptomic biomarker (Supplementary Fig. S7). The distributions of selection frequencies indicated that limited number of genes were frequently used in the marker. The numbers of highly selected genes with a selection frequency of 0.95 or higher were 140 for JA and 95 for SA. The highly selected genes included genes known as SA/JA responsive genes. ,The highly selected genes for JA included *JAZ1*, *JAZ2*, *JAZ3*, *JAZ5*, *JAZ6*, *LOX2*, and *ATGSTU1*. The highly selected genes for SA included *ZAR 1*, *WRKY18*, *WRKY70*, *ROXY18*, *ECS1*, and *ARR4* (Supplementary Table 3).

As a use case of the transcriptomic biomarker of the SA/JA response state, we investigated the responses to SA/JA in *npr3/4* double mutants: *npr3-1npr4-3* and *npr3-2npr4-2* (Fig. 6, Supplementary Fig. S6). We obtained transcriptome data of 87 samples for *npr3-1npr4-3* and 107 samples for *npr*3-*2npr4-2* at 25 conditions of SA and JA combining 5 concentrations. By applying transcriptomic biomarker to the transcriptome data, we estimated the SA/JA response state of *npr3/4* double mutants (Fig. 6). The mutants showed significantly higher predicted SA concentration than that in Col-0 for all SA treatment conditions except 1 mM SA (Fig. 6C, D). In other words, the mutants seemed to have a higher sensitivity to SA than Col-0. These results suggested that NPR3/4 suppressed the SA signaling pathway in conditions with lower than 1mM SA. These results were consistent with previous studies showing that NPR3 and NPR4 acted as transcriptional co-repressors of SA-responsive genes (Ding et al., 2018; Fu et al., 2012). On the other hand, when we focused on responses to JA, we found significant differences between mutants and Col-0 in several conditions (Fig. 6A, B).

However, the responses were not consistent among mutant alleles.

DISCUSSION

Our systematic analysis combining phytohormone treatments with large-scale transcriptome profiling has provided novel hypotheses and insights into SA/JA concentration-dependent responses. For instance, *CYP94B3* expression increased in a JA dose-dependent manner and enhanced at high SA concentrations (Fig. 1D, F). The 12-OH-JA-Ile produced by CYP94B3 exhibits weaker JA signaling compared to the JA-Ile (Saito et al., 2023). The decreased expression of JA-responsive downstream genes, such as *VSP1* and cluster A-02, coincided with the increased expression of *CYP94B3*. Attenuation of the JA pathway by CYP94B3 relieves suppression of the SA pathway, consequently enhancing resistance against *Pseudomonas syringae* pv. tomato DC3000 (Aubert et al., 2015; Hwang and Hwang, 2010). These findings suggest that JA-Ile oxidation by CYP94B3 has a role in SA-mediated defense response triggered by high SA concentrations induced during infection. Additionally, JA dose-dependent expression of *CYP94B3* indicates a mechanism to prevent excessive oxidation of JA-Ile. Although an SA concentration-dependent transcriptional regulation model involving NPR1/NPR3/NPR4 has been proposed (Ding et al., 2018; Fu et al., 2012), the combined SA and JA concentration-dependent regulation of transcription remains unclear. Further investigation is required to understand the transcriptional regulatory mechanisms triggered by the concentrations of SA/JA, such as *CYP94B3*.

We identified that combinations of SA/JA concentrations control most genes that share a biological function. The peak expression of indole GSL biosynthesis-related genes was detected at 30-fold higher JA concentrations than aliphatic GSL biosynthesis-related genes (Fig. 3B). Indole-3-carbinol and indole-3-acetonitrile, breakdown products from indole GSL, primarily inhibit pathogen growth (Aires et al., 2009; Madloo et al., 2021). Feeding damage to leaves provides entry points for pathogenic bacteria (Grode et al., 2017; Savatin et al., 2014). High concentrations of JA accumulating around damaged cells (Glauser et al., 2009) suggests the production of indole GSL to prevent secondary damage caused by

pathogens. In contrast, sulforaphane, a breakdown product from aliphatic GSL, negatively affects a wide variety of herbivores (Jeschke et al., 2016). JA accumulation is quantitatively lower in undamaged leaves compared to damaged ones (Ohnmeiss et al., 1997). Relatively low concentrations of JA likely enhance the synthesis of aliphatic GSL, inhibiting subsequent insect feeding. JA concentrations may be critical for inducing different types of GSLs in damaged and undamaged tissues to counteract the specific natural enemies anticipated in each tissue.

Although in this study we quantified the response of Arabidopsis seedlings to a wide range of SA/JA concentrations and combinations, the data from this study are still insufficient to elucidate the entire picture of the SA/JA responses. Tissue-specific and cell-type-specific responses could be overlooked because the whole seedling was used as the sample for RNA-Seq. Our measurement of total RNA amounts of shoot and root indicated that approximately 70% of total RNA of seedling was derived from shoot and 30% from root (Supplementary Fig. S8A). Responses of root-specific highly expressed genes were successfully measured (Supplementary Fig. S8B). However, if a gene that is expressed in both shoot and root shows opposite responses in shoot and root, the responses would be offset and undetectable. Specific responses in minor cell types would also be undetectable. Combining systematic SA/JA treatment with single-cell RNA-Seq analysis would help overcome these limitations. In addition to such tissue-specific responses, the influence of other hormones on SA/JA responses could be overlooked in our analysis. For example, abscisic acid, ethylene, brassinosteroid modulates SA and JA signaling pathways (Basit et al., 2021; Gupta et al., 2024; Li et al., 2019). Transcriptome profiling on combinatorial concentration treatments with other phytohormones is needed to quantitatively clarify a broader phytohormone signaling network. The throughput of our transcriptome profiling on combinatorial concentration treatments is enough high to expand the approach of this study to interactions between multiple phytohormones.

The transcriptomic biomarker that we developed in this study to predict SA/JA response status is expected to have a variety of applications. It is important to quantitatively evaluate the response states for multiple phytohormones (Pan and Wang, 2009; Šimura et al., 2018). Phytohormone quantification by mass spectrometry has been intensively developed and achieved very high sensitivity and accuracy (Kojima and Sakakibara, 2012; Petřík et al., 2024). It is suggested that for some reasons, the measured phytohormone levels do not always correspond to the response states (Vrobel and Tarkowski, 2023). Possible factors contributing to this discrepancy include receptor sensitivity, interactions among hormone signaling pathways and difficulty in distinguishing biologically active hormones from inactive conjugates. Complementary use of our transcriptomic biomarkers and the hormone quantifications will help to elucidate how this discrepancy arises. The transcriptomic biomarkers could be applicable to large-scale transcriptome data in emerging research areas: single-cell transcriptomics and field transcriptomics. A study combining single-nucleus RNA-Seq and spatial transcriptomics to analyze plant immune responses has been reported recently (Nobori et al., 2025). Applying the transcriptomic biomarkers to such datasets would reveal SA/JA response dynamics during plant immune responses at a single-cell resolution. In field transcriptomics, large amounts of transcriptome data acquired in the outdoor field are modeled with meteorological data to reveal the responses of organisms in real environments (Nagano et al., 2012). Large-scale field transcriptome studies consisting of hundreds or thousands of samples over several years have been reported in recent years (Hashida et al., 2024; Kashima et al., 2021; Nagano et al., 2019). Integrating the field transcriptome studies with SA/JA transcriptomic biomarkers would facilitate a systematic analysis of the interactions among climate factors and plant defense responses.

MATERIALS AND METHODS

Plant materials and SA/JA treatment

We used *Arabidopsis thaliana* (Col-0: CS70000, *npr3-1npr4-3*: CS72351 and *npr3-1npr4-3*: CS72352) to analyze the responses to SA & JA concentrations. The seeds of these lines were obtained from the Arabidopsis Biological Resource Center. Methyl jasmonate (135-14411, FUJIFILM Wako, Osaka, Japan) and sodium salicylate (S3007, Merck, Darmstadt, Germany) were dissolved to 1 M in ethanol or water, respectively. 100× SA or 100× JA stock solutions were then diluted from 1 M stock to 0 mM, 0.1 mM, 0.33 mM, 1 mM, 3.3 mM, 10 mM, 33 mM, and 100 mM in ethanol or water, respectively. Sixty-four variations of 50× SA/JA mixed stock solutions were prepared by combining eight concentrations of 100× SA and 100× JA, and mixing equal amounts of each. These 64 stock solutions for SA/JA treated samples, 50% EtOH in 1/2 MS medium for mock samples, and only 1/2 MS medium for untreated samples were transferred to a 96-well plate, and stored at −20°C until use. A single sterilized seed was sown in each well of 96-well plates and grown in 50 μL of liquid 1/2 MS medium. After 3 days of treatment at 4°C in the dark, the plants were cultivated at 20 °C for 5 days under continuous light. SA/JA treatments were performed by adding 2 μL of 50× SA/JA mixed stock solutions and 48 μL of liquid 1/2 MS medium to each well containing 5-day-old seedlings. This allowed the 5-day-old seedlings to be incubated for 6 h under 64 variations of SA and JA concentration conditions (Fig. 1A). To monitor the broad spectrum of early defense responses, we treated with SA/JA for 6 h ((Hou et al., 2024; McGrath et al., 2005)). Mock and untreated samples were treated for same time as above using 1% ethanol in 1/2 MS medium and only 1/2 MS medium, respectively. Four replicates of the plant were treated by each SA & JA condition, respectively. We removed the medium and added 100 μL of direct-RT buffer (Kashima et al., 2022) and a zirconia bead (YTZ-4, AS-ONE, Japan) to each well. Samples were ground using the TissueLyser II (QIAGEN, MD, USA) by 2 rounds

for 1.5 minutes of 2.5 Hz. The homogenates were centrifuged at 3000 rpm for 10 min, and 50 μL of the supernatants were stored as lysates at -20 °C. For test data of the transcriptomic biomarkers of SA/JA response state, we performed the same procedure using Col-0, *npr3-1npr4-3* and *npr3-1npr4-3* under twenty-five SA & JA concentration conditions made by combining five concentrations: 0 mM, 0.001 mM, 0.01 mM, 0.1 mM and 1 mM (Supplementary Fig. S6).

RNA-Seq experiment and basic data analysis

The 5 μL of lysate was used by RNA-Seq library preparation with the Lasy-seq v1.1 method (Kamitani et al., 2019). The library was sequenced by HiSeqX (Illumina, San Diego, CA) with the paired-end 150+150bp mode. Trimomatic v0.3.3 (Bolger et al., 2014) was used for trimming read data, and bowtie v1.1.2 (Langmead and Salzberg, 2012) and RSEM v1.3.0 (Li and Dewey, 2011)were used for expression quantification. For the following analysis, we used log2(rpm+1) values calculated by the same procedure of the previous study (Kamitani et al., 2019). The expression topography of all SA/JA responsive genes is shown in Supplementary Figure S9.

We excluded samples with fewer than $10^{5.5}$ total reads from the analysis (Supplementary Fig. S1A, B). We defined genes with more than 1.5 average $\log_2$ (RPM+1) as the expressed genes (Supplementary Fig. S1A, C). We calculated the standard deviation (SD) of the SA/JA-treated and control samples using the following procedure. To eliminate the effect of differences in sample numbers, 63 samples were randomly selected from each of the SA/JA-added samples and control samples. We calculated standard deviations among the 63 SA/JA-added samples as $SD_{treated}$ and standard deviations among the 63 control samples as $SD_{control}$. In the expressed genes, SA/JA responsive genes (3,001 genes in 370 samples) were selected based on the ratio of the $SD_{treated}$ to $SD_{control}$ (Supplementary Fig. S1D).

We detected differentially expressed genes between the control and each

concentration treatment using a likelihood ratio test of the edgeR package (Robinson et al., 2010). 0 mM SA and 0 mM JA, mock and untreated conditions were used as control samples. Expression data were normalized by TMM (Robinson and Oshlack, 2010). The FDR was controlled using Benjamini and Hochberg's method (Benjamini and Hochberg, 1995).

Expression Topography

The average expression levels were calculated for each condition. The average expression levels of 8 × 8 conditions data for each gene were designated as an expression topography. Smoothing by a 3 × 3 moving average filter was applied to the expression topography. Z-scores of the smoothed expression data were calculated using the scale function of R. Using the apcluster v.1.4.8 package (Bodenhofer et al., 2011), clustering was performed by the affinity propagation method based on Z-scores of the smoothed expression data. Pearson's correlation coefficient (r) was calculated using the Z-scores averaged over each cluster of affinity propagation. Groups of clusters were determined by hierarchical clustering. The correlation coefficients were as the distance between clusters, and the optimal number of groups was estimated by the gap statistic (Fig. 2C). Gene Ontology annotations were obtained from The Arabidopsis Information Resource (TAIR) on June 29, 2021. Fisher's exact test was used to test the enrichment of GO terms. The multiple testing correction was performed with a FDR. For these analyses, R 3.6.0 and 4.2.0 were used (R Core Team, 2024).

Transcriptomic biomarker of SA/JA response state

To create transcriptomic biomarkers correlated specifically with SA or JA, we employed the method using ensemble learning and L1-regularized linear regression (Fukuda et al., 2018) (Fig. 5A). Expression data of the 12,963 expressed genes from 370 samples in 64 concentration conditions were used as training data. The 1,296 genes, 10% of the expressed genes, were randomly selected and used as input variables for LASSO (Tibshirani, 1996). The

hyperparameter λ of LASSO was determined by cross-validation. The selection of subset of genes and LASSO were repeated 1,000 times. The median of the predicted values of the 1,000 regression models was used as the transcriptomic biomarker. Gene selection frequency was defined as the proportion of trials in which the gene had non-zero coefficient out of trials in which the gene was used as input variable (Supplementary Fig. S7). The test data of regression models were transcriptome data at 25 conditions of SA and JA combining 5 concentrations: 0, 0.001, 0.01, 0.1, and 1 mM. Analyses were performed using the glmnet package of R (R Core Team, 2024).

COMPETING INTERESTS

The authors declare that they have no competing interests.

FUNDING

This work was supported by JST CREST JPMJCR15O2, JST FOREST JPMJFR210B, JSPS (JP20H00423, JP23H00386, JP23K18156) and MEXT (JP23H04967) for AJN.

AUTHOR'S CONTRIBUTIONS

AJN and SB conceived the study. YN, YK and MK developed the assay system. AT and NMM conducted the RNA-Seq experiments. AT, TM and AJN analyzed the data. AT, and AJN wrote the manuscript with input from all co-authors.

ACKNOWLEDGEMENTS

We thank Dynacom Co., Ltd. (Chiba, Japan) for technical assistance with the analysis of RNA-Seq data.

DISCLOSURES

Conflicts of interest: No conflicts of interest declared.

DATA AVAILABLITY

The RNA-Seq data were submitted to the NCBI Sequence Read Archive repository under the BioProject PRJNA1232845. R scripts and data used in the analysis (count data, etc.) are available via the Dryad repository (https://doi.org/10.6084/m9.figshare.29163845.v1).

REFERENCES

Abuyusuf, M., Rubel, M.H., Kim, H.T., Jung, H.J., Nou, I.S., Park, J.I., 2023. Glucosinolates and Biotic Stress Tolerance in Brassicaceae with Emphasis on Cabbage: A Review. *Biochem Genet*, 61, 451–470. https://doi.org/10.1007/S10528-022-10269-6

Aires, A., Mota, V.R., Saavedra, M.J., Monteiro, A.A., Simões, M., Rosa, E.A.S., Bennett, R.N., 2009. Initial in vitro evaluations of the antibacterial activities of glucosinolate enzymatic hydrolysis products against plant pathogenic bacteria. *J Appl Microbiol*, 106, 2096–2105. https://doi.org/10.1111/J.1365-2672.2009.04181.X

Aubert, Y., Widemann, E., Miesch, L., Pinot, F., Heitz, T., 2015. CYP94-mediated jasmonoyl-isoleucine hormone oxidation shapes jasmonate profiles and attenuates defence responses to Botrytis cinerea infection. *J Exp Bot*, 66, 3879–3892. https://doi.org/10.1093/JXB/ERV190

Basit, F., Liu, J., An, J., Chen, M., He, C., Zhu, X., Li, Z., Hu, J., Guan, Y., 2021. Brassinosteroids as a multidimensional regulator of plant physiological and molecular responses under various environmental stresses. *Environ Sci Pollut Res Int*, 28, 44768–44779. https://doi.org/10.1007/S11356-021-15087-8

Benjamini, Y., & Hochberg, Y., 1995. Controlling the False Discovery Rate: A Practical and Powerful Approach to Multiple Testing. *J R Stat Soc Series B Stat Methodol*. Series B Methodological, 57(1), 289–300. https://doi.org/10.1111/j.2517-6161.1995.tb02031.x

Bjornson, M., Kajala, K., Zipfel, C., Ding, P., 2020. Low-cost and High-throughput RNA-seq Library Preparation for Illumina Sequencing from Plant Tissue. *Bio Protoc*, 10. https://doi.org/10.21769/BIOPROTOC.3799

Bodenhofer, U., Kothmeier, A., Hochreiter, S., 2011. APCluster: an R package for affinity propagation clustering. *Bioinformatics*, 27, 2463 – 2464. https://doi.org/10.1093/bioinformatics/btr406

Bolger, A.M., Lohse, M., Usadel, B., 2014. Trimmomatic: a flexible trimmer for Illumina sequence data. *Bioinformatics*, 30, 2114–2120. https://doi.org/10.1093/BIOINFORMATICS/BTU170

Chauvin, A., Lenglet, A., Wolfender, J.L., Farmer, E.E., 2016. Paired Hierarchical Organization of 13-Lipoxygenases in Arabidopsis. *Plants*, 2016, Vol. 5, Page 16 5, 16. https://doi.org/10.3390/PLANTS5020016

Ding, Y., Sun, T., Ao, K., Peng, Y., Zhang, Yaxi, Li, X., Zhang, Yuelin, 2018. Opposite Roles of Salicylic Acid Receptors NPR1 and NPR3/NPR4 in Transcriptional Regulation of Plant Immunity. *Cell*, 173, 1454-1467.e10. https://doi.org/10.1016/j.cell.2018.03.044

Dodds, P.N., Rathjen, J.P., 2010. Plant immunity: towards an integrated view of plant–pathogen interactions. *Nature Reviews Genetics*, 2010 11:8 11, 539–548. https://doi.org/10.1038/nrg2812

Fernández-Calvo, P., Chini, A., Fernández-Barbero, G., Chico, J.-M., Gimenez-Ibanez, S., Geerinck, J., Eeckhout, D., Schweizer, F., Godoy, M., Franco-Zorrilla, J.M., Pauwels, L., Witters, E., Puga, M.I., Paz-Ares, J., Goossens, A., Reymond, P., De Jaeger, G., Solano, R., 2011. The Arabidopsis bHLH Transcription Factors MYC3 and MYC4 Are Targets of JAZ Repressors and Act Additively with MYC2 in the Activation of Jasmonate Responses. *Plant Cell*, 23, 701–715. https://doi.org/10.1105/TPC.110.080788

Fritz, V.A., Justen, V.L., Bode, A.M., Schuster, T., Wang, M., 2010. Glucosinolate enhancement in cabbage induced by jasmonic acid application. *HortScience*, 45, 1188–

1191. https://doi.org/10.21273/HORTSCI.45.8.1188

Fu, Z.Q., Yan, S., Saleh, A., Wang, W., Ruble, J., Oka, N., Mohan, R., Spoel, S.H., Tada, Y., Zheng, N., Dong, X., 2012. NPR3 and NPR4 are receptors for the immune signal salicylic acid in plants. *Nature*, 486, 228–232. https://doi.org/10.1038/nature11162

Fukuda, A., Hirose, T., Aoki, N., Kondo, S., Yonekura, M., Kataoka, T., Ohto, C., Nagano, A.J., 2018. Selection of transcripts affecting initial growth rate of rice backcrossed inbred lines using RNA sequencing data. *Front Plant Sci*, 871, 414795. https://doi.org/10.3389/FPLS.2018.01880

Ghorbel, M., Brini, F., Sharma, A., Landi, M., 2021. Role of jasmonic acid in plants: the molecular point of view. *Plant Cell Reports*, 2021 40:8 40, 1471–1494. https://doi.org/10.1007/S00299-021-02687-4

Glauser, G., Dubugnon, L., Mousavi, S.A.R., Rudaz, S., Wolfender, J.L., Farmer, E.E., 2009. Velocity estimates for signal propagation leading to systemic jasmonic acid accumulation in wounded Arabidopsis. *Journal of Biological Chemistry*, 284, 34506–34513. https://doi.org/10.1074/jbc.M109.061432

Grode, A., Chen, S., Walker, E.D., Szendrei, Z., 2017. Onion Thrips (Thysanoptera: Thripidae) Feeding Promotes Infection By Pantoea ananatis in Onion. *J Econ Entomol*, 110, 2301–2307. https://doi.org/10.1093/JEE/TOX273

Guo, R., Shen, W., Qian, H., Zhang, M., Liu, L., Wang, Q., 2013. Jasmonic acid and glucose synergistically modulate the accumulation of glucosinolates in Arabidopsis thaliana. *J Exp Bot*, 64, 5707–5719. https://doi.org/10.1093/JXB/ERT348

Gupta S, Kaur R, Upadhyay A, Chauhan A, Tripathi V., 2024. Unveiling the secrets of abiotic

stress tolerance in plants through molecular and hormonal insights. *3 Biotech*. (10):252. https://doi.org/10.1007/s13205-024-04083-7

Hashida, Y., Kyogoku, D., Tanaka, S.E., Mori, N., Tanabata, T., Watanabe, H., Nagano, A.J., 2024. Field-crop transcriptome models are enhanced by measurements in systematically controlled environments. *bioRxiv*, 2024.09.21.614268. https://doi.org/10.1101/2024.09.21.614268

Hickman, R., Mendes, M.P., Verk, M.C. Van, Dijken, A.J.H. Van, Sora, J. Di, Denby, K., Pieterse, C.M.J., Wees, S.C.M. Van, 2019. Transcriptional Dynamics of the Salicylic Acid Response and its Interplay with the Jasmonic Acid Pathway. *bioRxiv*, 742742. https://doi.org/10.1101/742742

Hopkins, R.J., van Dam, N.M., van Loon, J.J.A., 2009. Role of Glucosinolates in Insect-Plant Relationships and Multitrophic Interactions. *Annu Rev Entomol*, 54, 57-83. https://doi.org/10.1146/annurev.ento.54.110807.090623

Hou, S., Tsuda, K., 2022. Salicylic acid and jasmonic acid crosstalk in plant immunity. *Essays Biochem*, 66, 647–656. https://doi.org/10.1042/EBC20210090

Howe GA, Jander G., 2008. Plant immunity to insect herbivores. *Annu Rev Plant Biol*. 59:41-66. https://doi.org/10.1146/annurev.arplant.59.032607.092825

Hwang, I.S., Hwang, B.K., 2010. Role of the pepper cytochrome P450 gene cacyp450a in defense responses against microbial pathogens. *Planta*, 232, 1409–1421. https://doi.org/10.1007/S00425-010-1266-Y

Jain, D., Khurana, J.P., 2018. Role of Pathogenesis-Related (PR) Proteins in Plant Defense Mechanism. *Molecular Aspects of Plant-Pathogen Interaction*, 265–281.

https://doi.org/10.1007/978-981-10-7371-7_12

Javed, T., Wang, W., Yang, B., Shen, L., Sun, T., Gao, S.J., Zhang, S., 2025. Pathogenesis related-1 proteins in plant defense: regulation and functional diversity. *Crit Rev Biotechnol*. https://doi.org/10.1080/07388551.2024.2344583

Jeschke, V., Gershenzon, J., Vassão, D.G., 2016. A mode of action of glucosinolate-derived isothiocyanates: Detoxification depletes glutathione and cysteine levels with ramifications on protein metabolism in Spodoptera littoralis. *Insect Biochem Mol Biol*, 71, 37–48. https://doi.org/10.1016/J.IBMB.2016.02.002

Kamitani, M., Kashima, M., Tezuka, A., Nagano, A.J., 2019. Lasy-Seq: a high-throughput library preparation method for RNA-Seq and its application in the analysis of plant responses to fluctuating temperatures. *Sci Rep*, 9, 1–14. https://doi.org/10.1038/s41598-019-43600-0

Kashima, M., Kamitani, M., Nomura, Y., Hirata, H., Nagano, A.J., 2020. DeLTa-Seq: direct-lysate targeted RNA-Seq from crude tissue lysate. *bioRxiv*, 2020.09.15.299180. https://doi.org/10.1101/2020.09.15.299180

Kashima, M., Kamitani, M., Nomura, Y., Mori-Moriyama, N., Betsuyaku, S., Hirata, H., Nagano, A.J., 2022. DeLTa-Seq: direct-lysate targeted RNA-Seq from crude tissue lysate. *Plant Methods*, 18, 1–18. https://doi.org/10.1186/s13007-022-00930-x

Kashima, M., Sakamoto, R.L., Saito, H., Ohkubo, S., Tezuka, A., Deguchi, A., Hashida, Y., Kurita, Y., Iwayama, K., Adachi, S., Nagano, A.J., 2021. Genomic Basis of Transcriptome Dynamics in Rice under Field Conditions. *Plant Cell Physiol*. https://doi.org/10.1093/PCP/PCAB088

Kenton, P., Mur, L.A.J., Atzorn, R., Wasternack, C., Draper, J., 1999. (-)-Jasmonic acid accumulation in tobacco hypersensitive response lesions. *Molecular Plant-Microbe Interactions*, 12, 74–78. https://doi.org/10.1094/MPMI.1999.12.1.74

Kitaoka, N., Kawaide, H., Amano, N., Matsubara, T., Nabeta, K., Takahashi, K., Matsuura, H., 2014. CYP94B3 activity against jasmonic acid amino acid conjugates and the elucidation of 12-O-β-glucopyranosyl-jasmonoyl-l-isoleucine as an additional metabolite. *Phytochemistry*, 99, 6–13. https://doi.org/10.1016/J.PHYTOCHEM.2013.12.019

Kojima, M., Sakakibara, H., 2012. Highly sensitive high-throughput profiling of six phytohormones using MS-probe modification and liquid chromatography-tandem mass spectrometry. *Methods Mol Biol*, 918, 151–164. https://doi.org/10.1007/978-1-61779-995-2_11

Koo, A.J.K., Cooke, T.F., Howe, G.A., 2011. Cytochrome P450 CYP94B3 mediates catabolism and inactivation of the plant hormone jasmonoyl-L-isoleucine. *Proc Natl Acad Sci U S A*, 108, 9298–9303. https://doi.org/10.1073/pnas.1103542108

Langmead, B., Salzberg, S.L., 2012. Fast gapped-read alignment with Bowtie 2. *Nature Methods*, 2012 9:4 9, 357–359. https://doi.org/10.1038/nmeth.1923

Li, B., Dewey, C.N., 2011. RSEM: accurate transcript quantification from RNA-Seq data with or without a reference genome. *BMC Bioinformatics*, 2011 12:1 12, 1–16. https://doi.org/10.1186/1471-2105-12-323

Li, N., Han, X., Feng, D., Yuan, D., Huang, L.J., 2019. Signaling Crosstalk between Salicylic Acid and Ethylene/Jasmonate in Plant Defense: Do We Understand What They Are Whispering?. *International Journal of Molecular Sciences*. 2019, Vol. 20, Page 671 20, 671. https://doi.org/10.3390/IJMS20030671

Liu, L., Sonbol, F.M., Huot, B., Gu, Y., Withers, J., Mwimba, M., Yao, J., He, S.Y., Dong, X., 2016. Salicylic acid receptors activate jasmonic acid signalling through a non-canonical pathway to promote effector-triggered immunity. *Nat Commun*, 7, 1–10. https://doi.org/10.1038/ncomms13099

Madloo, P., Lema, M., Cartea, M.E., Soengas, P., 2021. Sclerotinia sclerotiorum Response to Long Exposure to Glucosinolate Hydrolysis Products by Transcriptomic Approach. *Microbiol Spectr*, 9. https://doi.org/10.1128/spectrum.00180-21

Maruri-López, I., Aviles-Baltazar, N.Y., Buchala, A., Serrano, M., 2019. Intra and Extracellular Journey of the Phytohormone Salicylic Acid. *Front Plant Sci*, 0, 423. https://doi.org/10.3389/FPLS.2019.00423

Mishina, T.E., Zeier, J., 2007. Pathogen-associated molecular pattern recognition rather than development of tissue necrosis contributes to bacterial induction of systemic acquired resistance in Arabidopsis. *Plant Journal*, 50, 500–513. https://doi.org/10.1111/J.1365-313X.2007.03067.X

Munné-Bosch, S., Müller, M., 2013. Hormonal cross-talk in plant development and stress responses. *Front Plant Sci*, 4, 76598. https://doi.org/10.3389/FPLS.2013.00529

Mur, L.A.J., Kenton, P., Atzorn, R., Miersch, O., Wasternack, C., 2006. The Outcomes of Concentration-Specific Interactions between Salicylate and Jasmonate Signaling Include Synergy, Antagonism, and Oxidative Stress Leading to Cell Death. *Plant Physiol*, 140, 249–262. https://doi.org/10.1104/PP.105.072348

Nagano, A.J., Kawagoe, T., Sugisaka, J., Honjo, M.N., Iwayama, K., Kudoh, H., 2019. Annual transcriptome dynamics in natural environments reveals plant seasonal adaptation. *Nat Plants*, 5, 74–83. https://doi.org/10.1038/s41477-018-0338-z

Nagano, A.J., Sato, Y., Mihara, M., Antonio, B.A., Motoyama, R., Itoh, H., Nagamura, Y., Izawa, T., 2012. Deciphering and prediction of transcriptome dynamics under fluctuating field conditions. *Cell*, 151, 1358–1369. https://doi.org/10.1016/j.cell.2012.10.048

Niu, D.-D., Liu, H.-X., Jiang, C.-H., Wang, Y.-P., Wang, Q.-Y., Jin, H.-L., Guo, J.-H., 2011. The Plant Growth–Promoting Rhizobacterium Bacillus cereus AR156 Induces Systemic Resistance in Arabidopsis thaliana by Simultaneously Activating Salicylate- and Jasmonate/Ethylene-Dependent Signaling Pathways. *Molecular Plant-Microbe Interactions*, 24, 533–542. https://doi.org/10.1094/mpmi-09-10-0213

Nobori, T., Monell, A., Lee, T.A., Sakata, Y., Shirahama, S., Zhou, J., Nery, J.R., Mine, A., Ecker, J.R., 2025. A rare PRIMER cell state in plant immunity. *Nature*. https://doi.org/10.1038/s41586-024-08383-z

Ohnmeiss, T.E., McCloud, E.S., Lynds, G.Y., Baldwin, I.T., 1997. Within-plant relationships among wounding, jasmonic acid, and nicotine implications for defence in Nicotiana sylvestris. *New Phytol*, 137, 441–452. https://doi.org/10.1046/J.1469-8137.1997.00845.X

Pan, X., Wang, X., 2009. Profiling of plant hormones by mass spectrometry. *Journal of Chromatography B*, 877, 2806–2813. https://doi.org/10.1016/J.JCHROMB.2009.04.024

Petřík, I., Hladík, P., Zhang, C., Pěnčík, A., Novák, O., 2024. Spatio-temporal plant hormonomics: from tissue to subcellular resolution. *J Exp Bot*, 75. https://doi.org/10.1093/JXB/ERAE267

Pieterse, C.M.J., Dicke, M., 2007. Plant interactions with microbes and insects: from molecular mechanisms to ecology. *Trends Plant Sci*, 12, 564–569. https://doi.org/10.1016/J.TPLANTS.2007.09.004

Pieterse, C.M.J., Ton, J., Van Loon, L.C., 2001. Cross-talk between plant defence signalling pathways: boost or burden? *AgBiotechNet 3*.

R Core Team, 2024. R: A Language and Environment for Statistical Computing. R Foundation for Statistical Computing, Vienna, Austria. https://www.R-project.org/.

Robert-Seilaniantz, A., Grant, M., Jones, J.D.G., 2011. Hormone crosstalk in plant disease and defense: More than just JASMONATE-SALICYLATE antagonism. *Annu Rev Phytopathol*, 49, 317–343. https://doi.org/10.1146/ANNUREV-PHYTO-073009-114447

Robinson, M.D., McCarthy, D.J., Smyth, G.K., 2010. edgeR: a Bioconductor package for differential expression analysis of digital gene expression data. *Bioinformatics*, 26, 139–140. https://doi.org/10.1093/BIOINFORMATICS/BTP616

Robinson, M.D., Oshlack, A., 2010. A scaling normalization method for differential expression analysis of RNA-seq data. *Genome Biol*, 11, 1–9. https://doi.org/10.1186/GB-2010-11-3-R25

Saito, R., Muto, T., Urano, H., Kitajima, T., Kato, N., Kwon, E., Ueda, M., 2023. (3R,7S) ‐ 12 ‐ Hydroxy ‐ jasmonoyl ‐ <scp>l</scp> ‐ isoleucine is the genuine bioactive stereoisomer of a jasmonate metabolite in Arabidopsis thaliana. *The Plant Journal*, 115, 709–723. https://doi.org/10.1111/tpj.16256

Santacruz, D., Enane, F.O., Fundel-Clemens, K., Giner, M., Wolf, G., Onstein, S., Klimek, C., Smith, Z., Wijayawardena, B., Viollet, C., 2022. Automation of high-throughput mRNA-seq library preparation: a robust, hands-free and time efficient methodology. *SLAS Discov*, 27, 140–147. https://doi.org/10.1016/j.slasd.2022.01.002

Savatin, D. V., Gramegna, G., Modesti, V., Cervone, F., 2014. Wounding in the plant tissue:

The defense of a dangerous passage. *Front Plant Sci*, 5, 111139. https://doi.org/10.3389/fpls.2014.00470

Schweiger, R., Heise, A.M., Persicke, M., Müller, C., 2014. Interactions between the jasmonic and salicylic acid pathway modulate the plant metabolome and affect herbivores of different feeding types. *Plant Cell Environ*, 37, 1574–1585. https://doi.org/10.1111/PCE.12257

Šimura, J., Antoniadi, I., Široká, J., Tarkowská, D., Strnad, M., Ljung, K., Novák, O., 2018. Plant Hormonomics: Multiple Phytohormone Profiling by Targeted Metabolomics. *Plant Physiol*, 177, 476–489. https://doi.org/10.1104/PP.18.00293

Spoel, S.H., Johnson, J.S., Dong, X., 2007. Regulation of tradeoffs between plant defenses against pathogens with different lifestyles. *Proc Natl Acad Sci U S A*, 104, 18842–18847. https://doi.org/10.1073/PNAS.0708139104

Spoel, S.H., Koornneef, A., Claessens, S.M.C., Korzelius, J.P., Van Pelt, J.A., Mueller, M.J., Buchala, A.J., Métraux, J.P., Brown, R., Kazan, K., Van Loon, L.C., Dong, X., Pieterse, C.M.J., 2003. NPR1 modulates cross-talk between salicylate- and jasmonate-dependent defense pathways through a novel function in the cytosol. *Plant Cell*, 15, 760–770. https://doi.org/10.1105/TPC.009159

Takahashi, H., Kanayama, Y., Zheng, M.S., Kusano, T., Hase, S., Ikegami, M., Shah, J., 2004. Antagonistic Interactions between the SA and JA Signaling Pathways in Arabidopsis Modulate Expression of Defense Genes and Gene-for-Gene Resistance to Cucumber Mosaic Virus. *Plant Cell Physiol*, 45, 803–809. https://doi.org/10.1093/PCP/PCH085

Thaler, J.S., Humphrey, P.T., Whiteman, N.K., 2012. Evolution of jasmonate and salicylate signal crosstalk. *Trends Plant Sci*, 17, 260–270.

https://doi.org/10.1016/j.tplants.2012.02.010

Tibshirani, R., 1996. Regression Shrinkage and Selection Via the Lasso. *Journal of the Royal Statistical Society*, Series B (Methodological) 58, 267–288. https://doi.org/10.1111/J.2517-6161.1996.TB02080.X

Tsuda, K., Sato, M., Stoddard, T., Glazebrook, J., Katagiri, F., 2009. Network properties of robust immunity in plants. *PLoS Genet*, 5. https://doi.org/10.1371/JOURNAL.PGEN.1000772

Van Wees, S.C.M., De Swart, E.A.M., Van Pelt, J.A., Van Loon, L.C., Pieterse, C.M.J., 2000. Enhancement of induced disease resistance by simultaneous activation of salicylate- and jasmonate-dependent defense pathways in *Arabidopsis thaliana*. *Proc Natl Acad Sci U S A*, 97, 8711–8716. https://doi.org/10.1073/pnas.130425197

Vrobel, O., Tarkowski, P., 2023. Can plant hormonomics be built on simple analysis? A review. *Plant Methods*, 19, 1–22. https://doi.org/10.1186/S13007-023-01090-2

Wasternack, C., Hause, B., 2013. Jasmonates: biosynthesis, perception, signal transduction and action in plant stress response, growth and development. An update to the 2007 review in Annals of Botany. *Ann Bot*, 111, 1021–1058. https://doi.org/10.1093/AOB/MCT067

Weech, M.H., Chapleau, M., Pan, L., Ide, C., Bede, J.C., 2008. Caterpillar saliva interferes with induced Arabidopsis thaliana defence responses via the systemic acquired resistance pathway. *J Exp Bot*, 59, 2437–2448. https://doi.org/10.1093/JXB/ERN108

Wittstock, U., Burow, M., 2010. Glucosinolate Breakdown in Arabidopsis: Mechanism, Regulation and Biological Significance. *Arabidopsis Book*, 8, e0134.

https://doi.org/10.1199/tab.0134

Yang, T.-H., Lenglet-Hilfiker, A., Stolz, S., Glauser, G., Farmer, E.E., 2020. Jasmonate Precursor Biosynthetic Enzymes LOX3 and LOX4 Control Wound-Response Growth Restriction. *Plant Physiol*, 184, 1172–1180. https://doi.org/10.1104/pp.20.00471

Zhang, N., Zhou, S., Yang, D., Fan, Z., 2020. Revealing Shared and Distinct Genes Responding to JA and SA Signaling in Arabidopsis by Meta-Analysis. *Front Plant Sci*, 11, 512053. https://doi.org/10.3389/FPLS.2020.00908

Zheng, X., Spivey, N.W., Zeng, W., Liu, P.-P., Fu, Z.Q., Klessig, D.F., He, S.Y., Dong, X., 2012. Coronatine Promotes *Pseudomonas syringae* Virulence in Plants by Activating a Signaling Cascade that Inhibits Salicylic Acid Accumulation. *Cell Host & Microbe*, 11, 587–596. https://doi.org/10.1016/j.chom.2012.04.014

Hou, J., Ai, M., Li, J., Cui, X., Liu, Y., Yang, Q., 2024. Exogenous salicylic acid treatment enhances the disease resistance of Panax vietnamensis by regulating secondary metabolite production. Front Plant Sci 15. https://doi.org/10.3389/FPLS.2024.1428272

McGrath, K.C., Dombrecht, B., Manners, J.M., Schenk, P.M., Edgar, C.I., Maclean, D.J., Scheible, W.R., Udvardi, M.K., Kazan, K., 2005. Repressor- and Activator-Type Ethylene Response Factors Functioning in Jasmonate Signaling and Disease Resistance Identified via a Genome-Wide Screen of Arabidopsis Transcription Factor Gene Expression. Plant Physiol 139, 949. https://doi.org/10.1104/PP.105.068544

FIGURE LEGENDS

Figure1 Treatments of 64 combinations of SA/JA concentrations

(A) SA/JA treatment for A. thaliana seedling using 96-well plates. Each sample was treated with SA and JA at 64 conditions that were systematically combined among 8 concentrations: 0 mM, 0.001 mM, 0.0033 mM, 0.01 mM, 0.033 mM, 0.1 mM, 0.33 mM, and 1 mM. (B) A 96-well plate with seedling just prior to the SA/JA treatment. (c - f) Expression topography of genes related SA/JA responses. The horizontal axis of the heatmap corresponds to the concentration of SA, and the vertical axis to the concentration of JA. The color of each cell indicates the average log2(RPM + 1) for each concentration condition, n = 3~11. PR1 is a marker gene for SA responses. (C). VSP1 is a marker gene for JA responses. (D). LOX3 is encoding enzymes involved in JA synthesis (E). CYP94B3 is involved in the downregulation of the JA response (F). (G - I) Principal component analysis of samples. Each point represents samples. The color of each point indicates the log-transformed SA concentration (G), JA concentration (H), and batch of the experiment (I).

Figure 2 Forty-three clusters of expression topography represent various SA/JA responses

(A) Average expression topography of each cluster. The horizontal axis is the concentration of SA, and the vertical axis is the concentration of JA. The colors represent the relative expression values of the genes in each cluster, with lighter colors indicating higher expression levels. (B) Upper 2 plots indicate concentration of SA/JA. Lower 2 plots show the relative expression levels of the cluster A-02 and cluster C-01. Expression profiles of 40 genes in cluster A-02 and 64 genes in cluster C-01 are indicated as gray points and lines. Mean expression is indicated as red lines. (C) Matrix of Pearson's correlation between the means of each cluster, sorted into eight groups by hierarchical clustering.

Figure 3 Genes with similar expression topographies were involved in same biological prosses.

(A) GO enrichment in the clusters. The number of genes contained in each cluster is indicated in parentheses. The size of the circles indicates the number of genes. The color scale indicates the adjusted P-value (FDR) in the GO enrichment analysis. At the bottom of panel, The expression topographies of the clusters are shown. The colors represent the relative expression values of the genes in each cluster, with lighter colors indicating higher expression levels. A full list of enriched GO terms was indicated in Supplemental Table 2. (B, C) Relative expression levels of glucosinolate (GSL) synthesis genes. Mean expressions for 0 - 0.01 mM SA conditions (B) or 0.033 - 1 mM SA conditions (C) are plotted. The horizontal axis indicates JA concentration (mM), and the vertical axis indicates relative expression level. Aliphatic GSL synthesis genes are shown in red. Indole GSL synthesis genes are shown in blue. Bold lines indicate LOESS curves drawn for each glucosinolate type. (D-G) Expression topographies of aliphatic GSL synthesis genes. (H-K) Expression topographies of indole GSL synthesis genes. Data used in the panel (B) are indicated by green boxes.

Figure 4 Correlation between expression of single gene and SA/JA concentrations.

(A, B) Histogram of correlation coefficients between gene expression levels and SA concentrations (A), JA concentration (B). (C) Scatter plot of correlation coefficients between gene expression levels and SA/JA concentrations. Genes with the highest or lowest correlation coefficient are indicated as points. (D-G) Expression topographies of genes with the highest positive and negative correlation. HRG2 with the highest positive correlation coefficient for SA concentration (D), and UL4Z with the highest negative correlation (E). *AT2G47950* with the highest positive correlation coefficient for JA concentration (F), and SAUR6 with the highest negative correlation (G).

Figure 5 Transcriptomic biomarker of SA/JA response state. (A) Scheme of development of a transcriptomic biomarker of SA/JA response state from RNA-seq data. See Materials and Methods for further details. (B, C) Predictions of the transcriptomic biomarkers for training data. Predicted value of the marker for SA response state and treated SA concentration (B). Predicted value of the marker for JA response state and treated JA concentration (C). (D-G) Predicted value of the transcriptomic biomarkers for test data of Col-0. Predicted value of the SA marker and treated SA concentration for test data (D). Predicted value of the JA marker and treated JA concentration for test data (E). Predicted value of the SA marker and treated JA concentration for test data (F). Predicted value of the JA marker and treated SA concentration for test data (G). The result of liner regression is shown in the blue line.

Figure 6 SA/JA response states of *npr3/4* double mutants. (A) Predictions of the JA marker for *npr3/4* double mutants. Data obtained from 25 concentration conditions were grouped by the treated SA concentrations. The vertical axis indicates the predicted SA concentrations by the transcriptomic biomarker. (B) Liner regression between the treated SA concentrations and the predicted SA concentrations. Formula for the liner regression was shown in the plot. (C) Predictions of the JA marker for *npr3/4* double mutants. Data obtained from 25 concentration conditions were grouped by the treated JA concentrations. The vertical axis indicates the predicted JA concentrations by the transcriptomic biomarker. (D) Liner regression between the treated JA concentrations and the predicted JA concentrations. Formula for the liner regression was shown in the plot. Results of Mann-Whitney's U test were indicated as *: $P < 0.05$, **: $P < 0.01$, ***: $P < 0.001$ and NS: not significant.

SUPPLEMENTARY MATERIAL

Supplementary figure S1 Sample and gene filtering of RNA-seq data

(A) Schematic flow of sample and gene filtering. (B) Histogram of total read counts for samples. (C) Histogram of average expression levels. Genes whose expressions were greater than 1.5 were defined as expressed genes. (D) Scatter plot of $SD_{treated}$ and $SD_{control}$. Genes whose ratio of $SD_{treated}$ to $SD_{control}$ were greater than 1.2 were defined as SA/JA responsive genes. Red lines indicate thresholds.

Supplementary Figure S2 Gene expression under combined SA/JA treatment.

(A-D) Scatter plot of gene expression levels under SA/JA treatment conditions (mM). Black circles represent log (RPM + 1) expression values for each individual RNA-seq sample. Upper panels of x-axis are SA concentration and JA fixed at the value indicated above each panel. Lower panels of x-axis are JA concentration and SA fixed at the value indicated above each panel. The orange line indicates LOESS curves, and the light-grey band shows the 95 % confidence interval.

Supplementary figure S3. Principal-component analysis of transcriptome samples.

(A) Scores of PC1 (19.3 % variance) plotted against log-transformed SA concentrations. The PC1 primarily captures SA dose-dependent effects. (B) Scores of PC2 (6.7 % variance) plotted against log-transformed JA concentrations. The PC2 primarily captures JA dose-dependent effects. (C–F) Pairwise combinations of the subsequent PCs (PC1–PC8) colored by 96-well plate number (Plate 1, red; Plate 2, green; Plate 3, blue; Plate 4, purple). The overlap among ellipses shows that the Top 8 PCs were not captured by plate-to-plate variation.

Supplementary figure S4 Number of differentially expressed genes by SA/JA treatment

The number of differentially expressed genes between the control group and other 63 SA/JA

treatment conditions (FDR = 0.05). (A) Number of genes that were up-regulated by SA/JA treatments. (B) Number of genes that were down-regulated by SA/JA treatments. (C) Number of genes that were differentially expressed by SA/JA treatments. (D) Difference between the number of up-regulated genes and the number down-regulated by SA/JA treatments.

Supplementary figure S5. Relative expression levels of GSL synthesis genes

(A-H) Relative expression levels of GSL synthesis genes at SA concentrations for 0 mM (A), 0.001 mM (B), 0.0033 mM (C), 0.01 mM (D), 0.033 mM (E), 0.1 mM (F), 0.33 mM (G), 1 mM (H). The horizontal axis indicates JA concentration (mM), and the vertical axis indicates relative expression level. Aliphatic GSL synthesis genes are shown in red. Indole GSL synthesis genes are shown in blue. Bold lines indicate LOESS curves drawn for each glucosinolate type.

Supplementary figure S6 Summary of test data of transcriptomic biomarkers for SA/JA response states (a-c) Layouts of SA treatment (A), JA treatment (B), and genotype (C) for test data. Seedlings were treated with SA and JA at 25 conditions that were made by systematically combining 5 concentrations of SA and JA: 0 mM, 0.001 mM, 0.01 mM, 0.1 mM, and 1 mM. (D-F) Principal component analysis of samples of test data. The color of each point indicates the genotypes (D), log-transformed SA concentrations (E) and JA concentrations (F).

Supplementary figure S7 Selection frequency of genes in the transcriptomic biomarker

(A) Scatter plot of selection frequency in the SA marker and JA marker. (B, C) Histogram of selection frequency in the SA marker (B) and JA marker (C).

Supplementary figure S8 Gene expressions of root-specific genes were detectable.

(A) The total RNA contents of seedlings, shoots and roots. Error bars represent the standard deviation (n = 12). (B) Expression topographies of genes expressed specifically and highly in roots (A Christ et al., 2013). The horizontal axis of the heatmap corresponds to the concentration of SA, and the vertical axis to the concentration of JA. The color of each cel indicates the average log2(RPM + 1) for each concentration condition, n = 3~11.

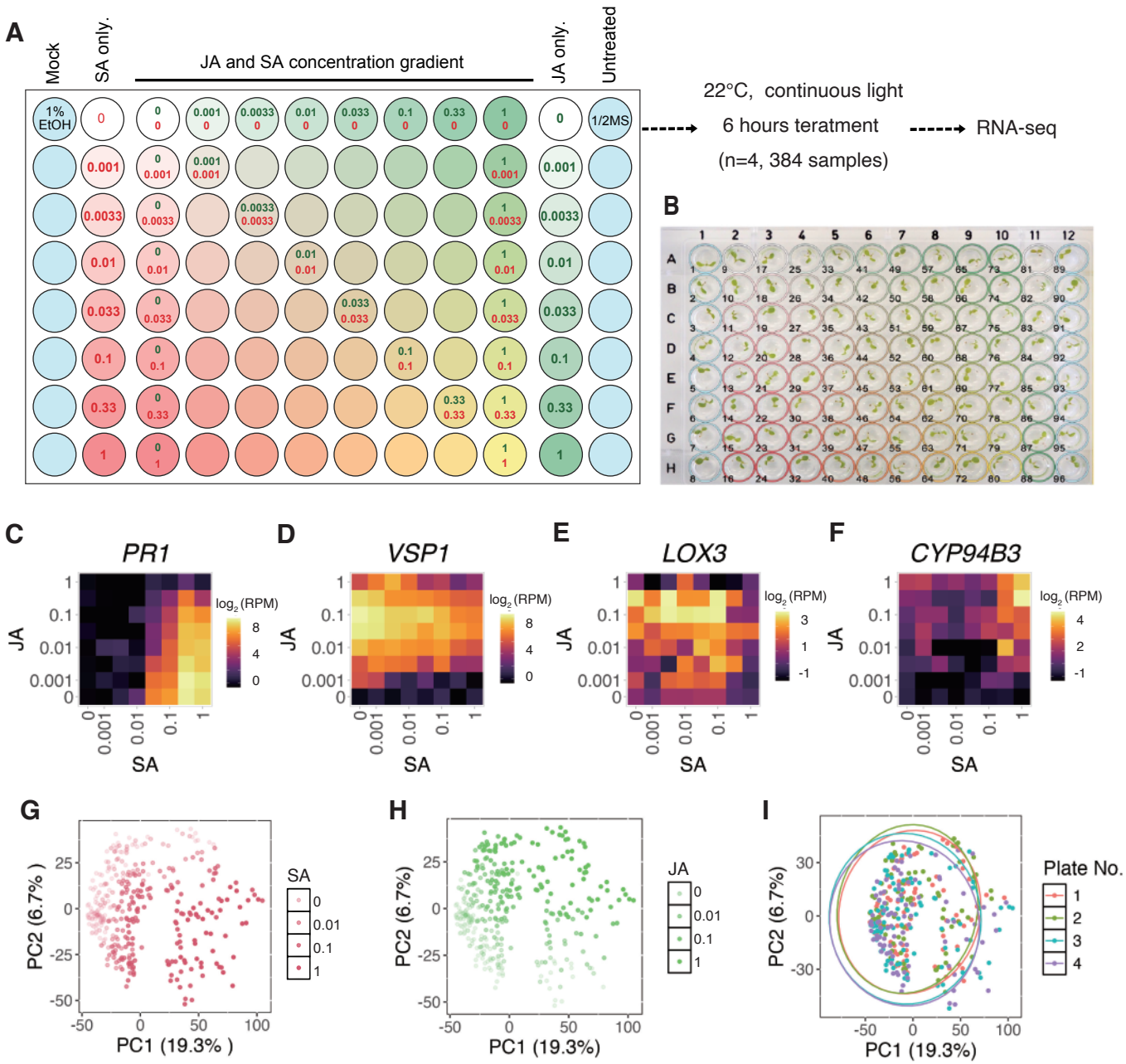

Figure1 Treatments of 64 combinations of SA/JA concentrations

(A) SA/JA treatment for *A. thaliana* seedling using 96-well plates. Each sample was treated with SA and JA at 64 conditions that were systematically combined among 8 concentrations: 0 mM, 0.001 mM, 0.0033 mM, 0.01 mM, 0.033 mM, 0.1 mM, 0.33 mM, and 1 mM. (B) A 96-well plate with seedling just prior to the SA/JA treatment. (C-F) Expression topography of genes related SA/JA responses. The horizontal axis of the heatmap corresponds to the concentration of SA, and the vertical axis to the concentration of JA. The color of each cell indicates the average log2(RPM + 1) for each concentration condition, n = 3~11. *PR1* is a marker gene for SA responses. (C). VSP1 is a marker gene for JA responses. (D). LOX3 is encoding enzymes involved in JA synthesis (E). CYP94B3 is involved in the downregulation of the JA response (F). (G - I) Principal component analysis of samples. Each point represents samples. The color of each point indicates the log-transformed SA concentration (G), JA concentration (H), and batch of the experiment (I).

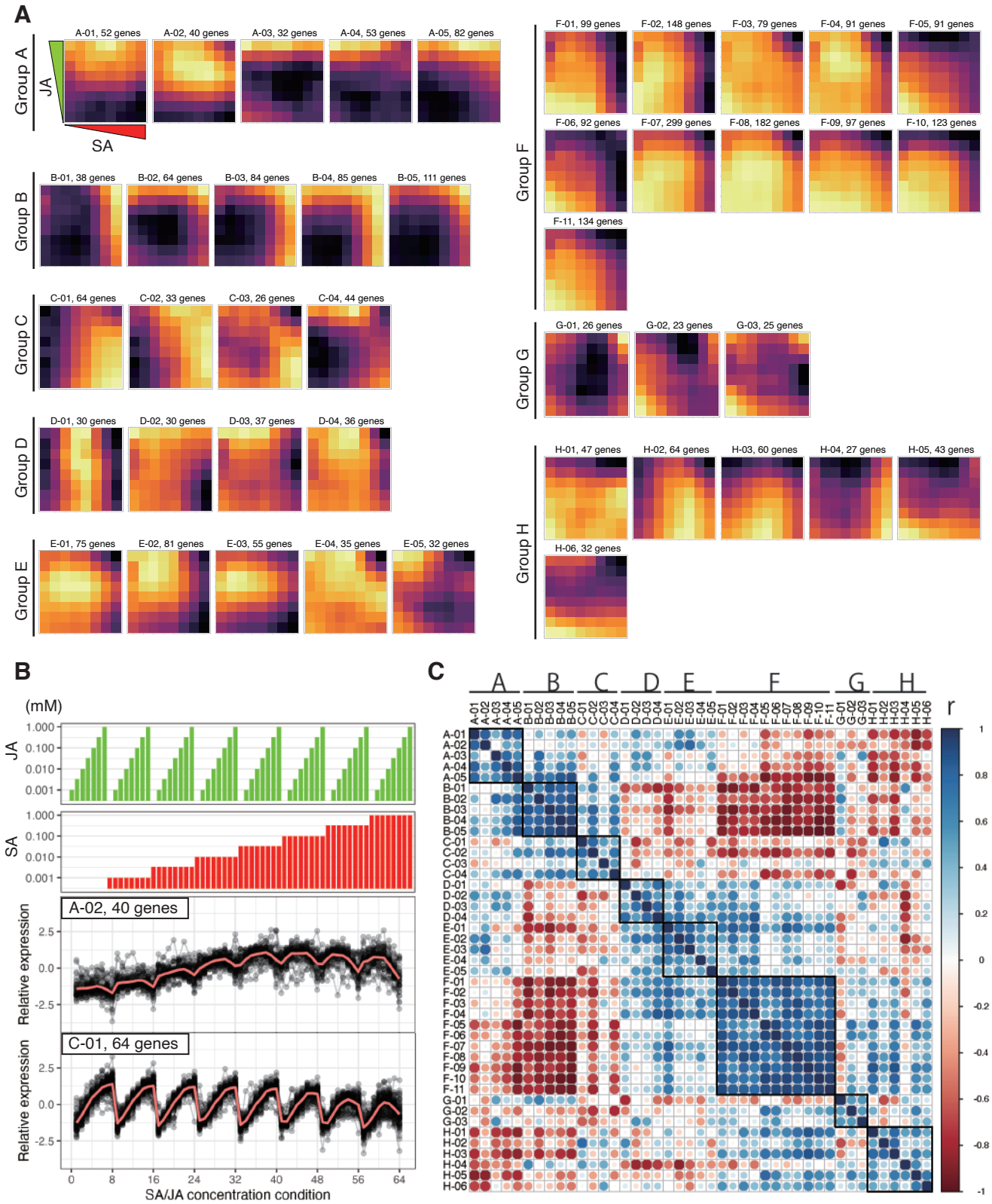

Figure 2 Forty-three AP clusters of expression topography represent various SA/JA responses

(A) Average expression topography of each cluster. The horizontal axis is the concentration of SA, and the vertical axis is the concentration of JA. The colors represent the relative expression values of the genes in each cluster, with lighter colors indicating higher expression levels. (B) Upper 2 plots indicate concentration of SA/JA. Lower 2 plots show the relative expression levels of the AP cluster A-02 and AP cluster C-01. Expression profiles of 40 genes in AP cluster A-02 and 64 genes in AP cluster C-01 are indicated as gray points and lines. Mean expression is indicated as red lines. (C) Matrix of Pearson's correlation between the means of each cluster, sorted into eight groups by hierarchical clustering.

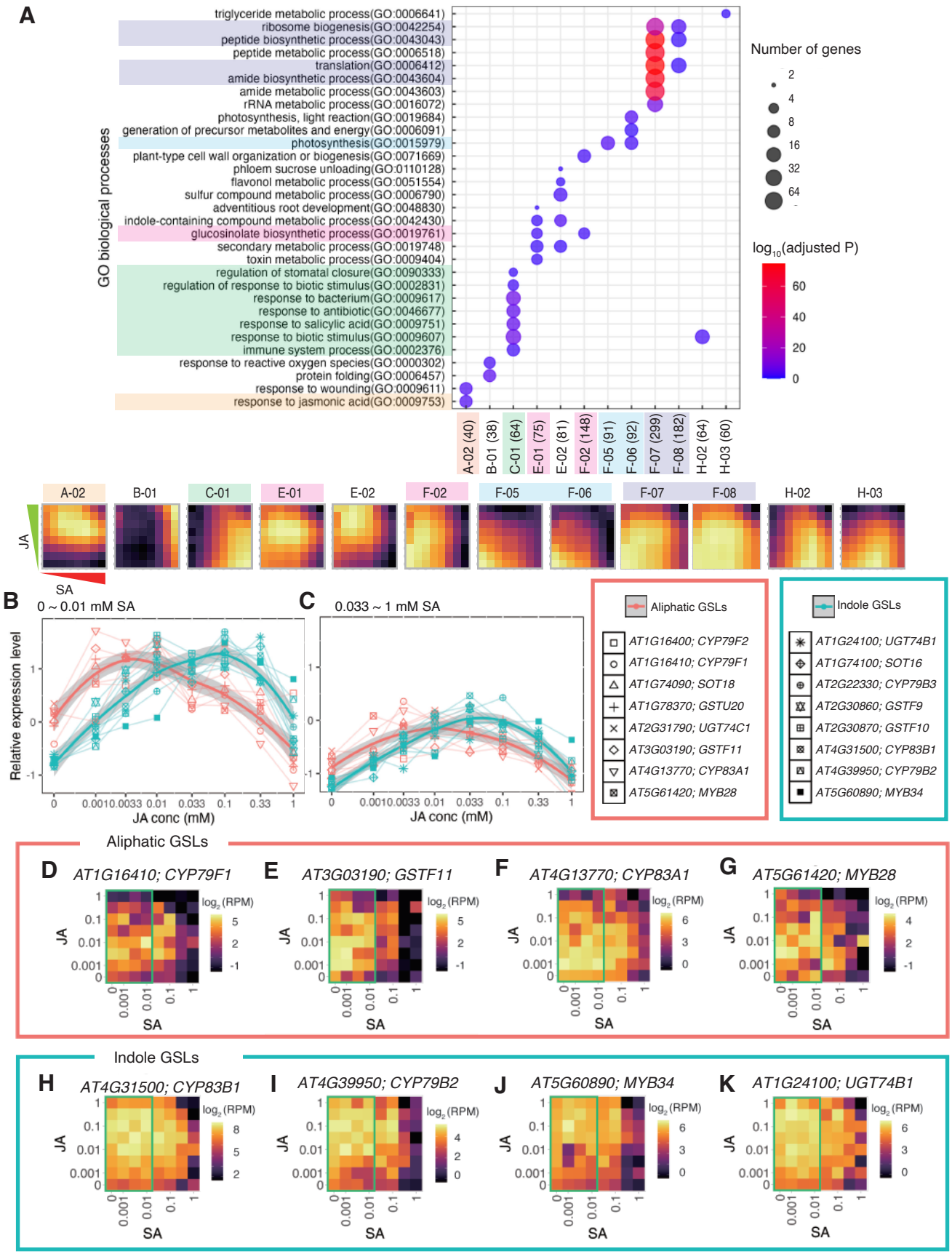

Figure 3 Genes with similar expression topographies were involved in same biological prosses.

(A) GO enrichment in the AP clusters. The number of genes contained in each cluster is indicated in parentheses. The size of the circles indicates the number of genes. The color scale indicates the adjusted P-value (FDR) in the GO enrichment analysis. The expression topographies of the AP clusters are shown. The colors represent the relative expression values of the genes in each cluster, with lighter colors indicating higher expression levels. A full list of enriched GO terms was indicated in Supplemental Table 1. (B, C) Relative expression levels of glucosinolate (GSL) synthesis genes. Mean expressions for 0 - 0.01 mM SA conditions (B) or 0.033 - 1 mM SA conditions (C) are plotted. The horizontal axis indicates JA concentration (mM), and the vertical axis indicates relative expression level. Aliphatic GSL synthesis genes are shown in red. Indole GSL synthesis genes are shown in blue. Bold lines indicate LOESS curves drawn for each glucosinolate type. (D-G) Expression topographies of aliphatic GSL synthesis genes; (D) AT1G16410, (E) AT3G03190, (F) AT4G13770 and (G) AT1G24100. (H-K) Expression topographies of indole GSL synthesis genes; (H) AT4G31500, (I) AT4G39950, (J) AT5G60890 and (K) AT5G61420. Data used in the panel (B) are indicated by green boxes.

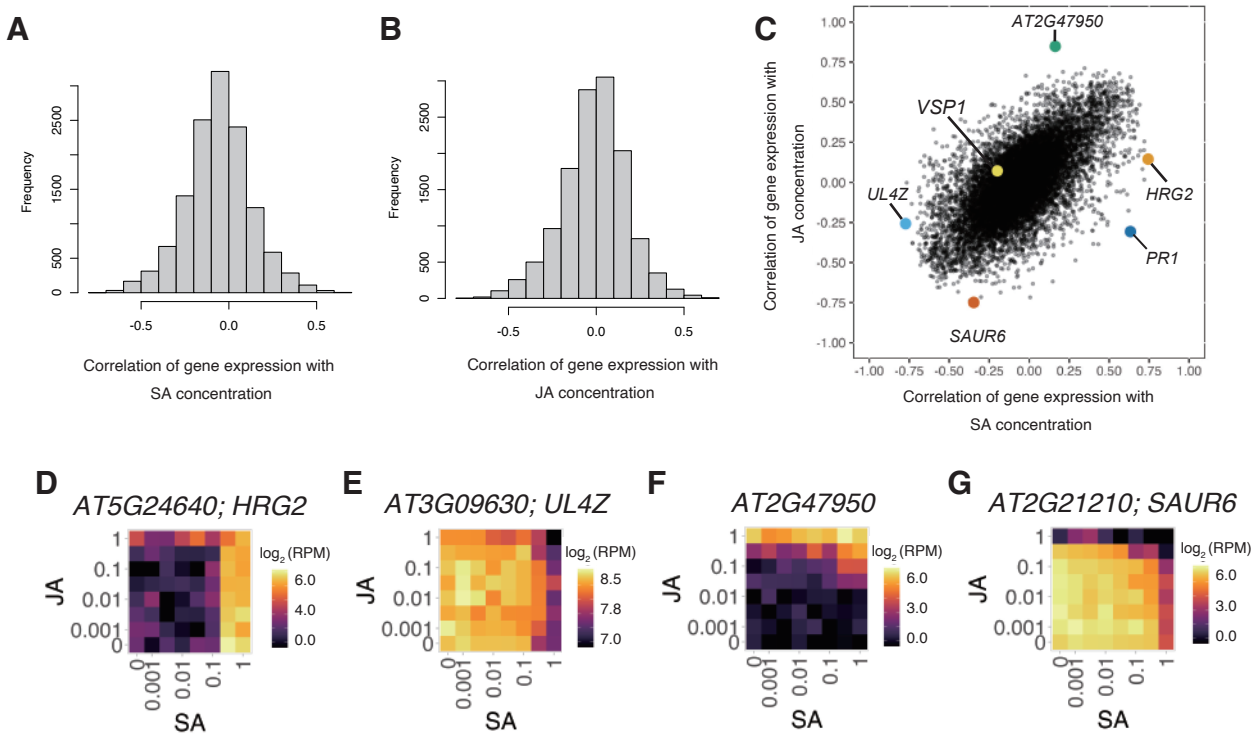

Figure 4 Correlation between expression of single gene and SA/JA concentrations

(A, B) Histogram of correlation coefficients between gene expression levels and SA concentrations (A), JA concentration (B). (C) Scatter plot of correlation coefficients between gene expression levels and SA/JA concentrations. Genes with the highest or lowest correlation coefficient are indicated as red points. (D-G) Expression topographies of genes with the highest correlation. *HRG2* with the highest or lowest correlation coefficient for SA concentration (D), and *UL4Z* with the lowest (E). *AT2G47950* with the highest correlation coefficient for JA concentration (F), and *SAUR6* with the lowest (G).

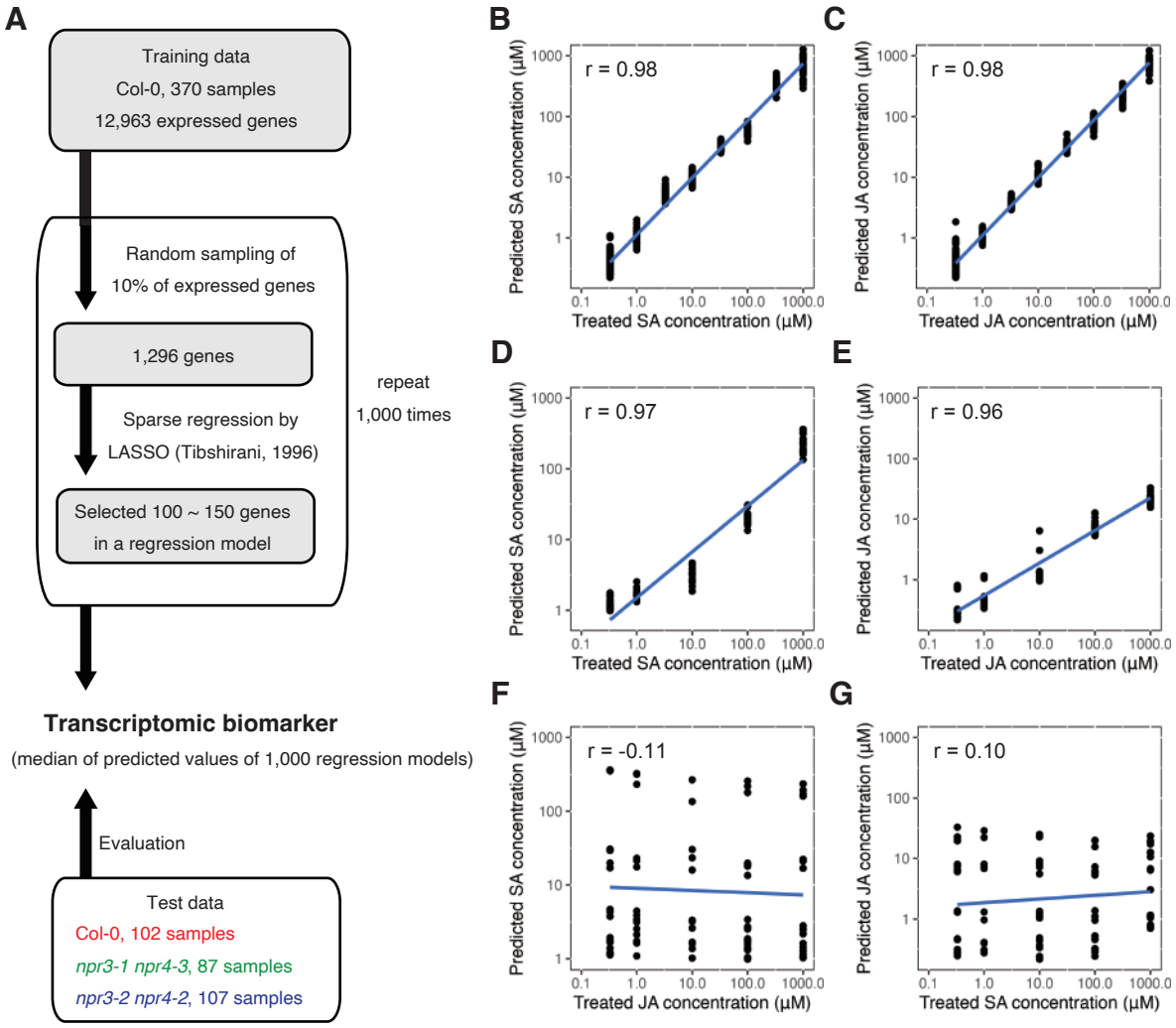

Figure 5 Transcriptomic biomarker of SA/JA response state

(A) scheme of development of a transcriptomic biomarker of SA/JA response state from RNA-seq data. See Materials and Methods for further details. (B, C) Predictions of the transcriptomic biomarkers for training data. Predicting of the marker for SA response state and treated SA concentration (B). Predicting of the marker for JA response state and treated JA concentration (C). (D-G) Predicting of the transcriptomic biomarkers for test data of Col-0. Prediction of the SA marker and treated SA concentration for test data (D). Prediction of the JA marker and treated JA concentration for test data (E). Prediction of the SA marker and treated JA concentration for test data (F). Prediction of the JA marker and treated SA concentration for test data (G). The horizontal axis is the predicted SA/JA concentration by the transcriptomic biomarker, and the vertical axis is the treated SA/JA concentration. The result of liner regression is shown in the blue line.

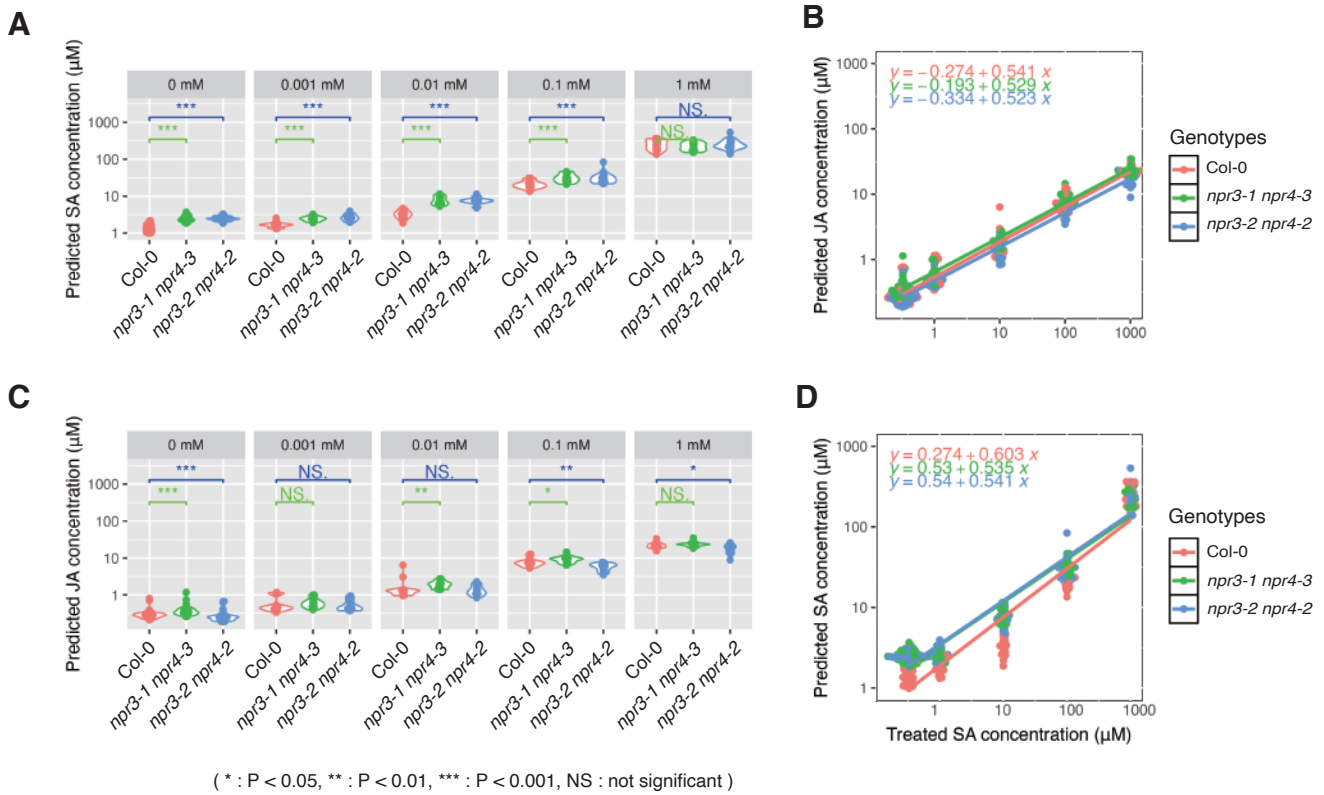

(* : P < 0.05, ** : P < 0.01, *** : P < 0.001, NS : not significant)

Figure 6 SA/JA response states of npr3/4 double mutants.

(A) Predictions of the JA marker for npr3/4 double mutants. Data obtained from 25 concentration conditions were grouped by the treated JA concentrations. The vertical axis indicates the predicted JA concentrations by the transcriptomic biomarker. (B) Liner regression between the treated JA concentrations and the predicted JA concentrations. Formula for the liner regression was shown in the plot. (C) Predictions of the SA marker for npr3/4 double mutants. Data obtained from 25 concentration conditions were grouped by the treated SA concentrations. The vertical axis indicates the predicted SA concentrations by the transcriptomic biomarker. (D) Liner regression between the treated SA concentrations and the predicted SA concentrations. Formula for the liner regression was shown in the plot. Results of Mann-Whitney's U test were indicated as *: P < 0.05, **: P < 0.01, ***: P < 0.001 and NS: not significant.